



Optimization of dewetting conditions for hollow fiber membranes in vacuum membrane distillation

Yonghyun Shin, Jihyuck Choi, Taewoong Lee, Jinsik Sohn, Sangho Lee*

Department of Civil and Environment Engineering, Kookmin University, Jeongneung-gil 77, Seongbuk-gu 136702, Seoul, Republic of Korea, Tel. +82 2 910 4529; Fax: +82 2 910 4939; email: sanghlee@kookmin.ac.kr (S. Lee)

Received 19 November 2014; Accepted 13 April 2015

ABSTRACT

Membrane distillation (MD) is a thermal separation process that uses a hydrophobic membrane as a barrier between a liquid phase and a gas phase. Accordingly, MD can only be applied under the conditions where the membrane is not wetted by the feed solution. In this study, a technique to remove water inside the pores of the wetted membranes, or “dewetting,” was developed to mitigate the problems of membrane wetting in MD process. High-temperature air was applied to the wetted membranes using a specially designed device. The dewetting efficiency was analyzed by measuring the liquid entry pressure, water flux, and salt rejection. The response surface methodology (RSM) was applied to explore the optimum conditions for dewetting of MD membranes. Results indicated that dewetting should be done under proper conditions. If the temperature and dewetting time were insufficient, the dewetting was incomplete. On the other hand, the membrane was partially deformed if the temperature was too high and the dewetting time was too long. Based on the RSM results, the optimum conditions for the temperature and time ranged from 60 to 70°C and from 8 to 12.5 min, respectively.

Keywords: Membrane distillation; Wetting; Dewetting; Liquid entry pressure; Response surface methodology

1. Introduction

Membrane distillation (MD) is a thermally driven separation process where a hydrophobic membrane acts a barrier against the liquid phase [1,2]. This membrane allows the vapor passage through the membrane pores and blocks the water penetration [3]. This process has been studied since the 1960s [4]. Development in membrane manufacturing in the 1980s allowed us to obtain commercial membranes

with desired properties [4]. Improvements in module design and better understanding of phenomena occurring in a layer adjacent to a membrane also contributed to renewed interest in MD.

There are many advantages in MD over conventional thermal distillation processes [3,5]. MD enables almost 100% rejection of ions, macromolecules, colloids, cells, and other nonvolatiles from the process stream [6]. MD also requires low operating temperatures and operating pressures, enabling the utilization of waste heat as a preferable energy source [7]. The

*Corresponding author.

possibility of utilizing of alternative energy sources such as solar or geothermal energy is particularly attractive [3].

Although MD has attracted significant attention as a potential technology for desalination of seawater and brackish water, it has critical problems associated with pore wetting [8,9]. When MD operates for a long time or in the presence of chemicals such as organic solvents and oil, feed water may penetrate into the pores of the membrane, leading to an abrupt decrease in flux and rejection. Accordingly, it is necessary to remove water inside the pores of the wetted membranes.

The pore wetting of the membranes is a complex phenomenon where physical and chemical interactions exist [10,11]. Due to the hydrophobic nature of the membrane, liquid water cannot penetrate into the pores of the membrane until the applied pressure exceeds the liquid entry pressure (LEP) [12]. The LEP is defined as the pressure difference from which the liquid penetrates into the pores of the hydrophobic membrane. This critical pressure difference is correlated to the interfacial tension, the contact angle of the liquid on the surface, and the size and shape of membrane pores. The chemical properties of the feed solution may change the interfacial tension, thereby affecting the degree of the wetting. It has been reported that membrane fouling is closely related to pore wettings [9,11].

Although the wetting of MD membranes is a serious problem to be overcome, little information is available on dewetting techniques to remove water inside the pores of the wetted membranes [9,13]. In this context, this study aimed at the development of dewetting method for MD membrane using hot air, which evaporates the water inside the wetted membrane. The effect of air temperature and exposure time

on the dewetting efficiency was investigated by comparing the LEP, water flux, and salt rejection. The response surface methodology (RSM) was also applied to optimize the conditions for dewetting.

2. Materials and methods

2.1. Membrane

Hollow-fiber membranes made of polyvinylidene fluoride (PVDF, Ecomity) were used for the experiments. The nominal pore size of the membranes was 0.22 μm . The inner diameter and outer diameter were 0.8 and 1.2 mm, respectively. A laboratory-scale membrane module with the effective membrane area of 0.0125 m^2 was prepared prior to the experiments.

2.2. Experimental setup

A laboratory-scale vacuum MD system was developed and used for measuring flux and rejection in MD operation, as illustrated in Fig. 1. The system consists of a hollow-fiber membrane module, a vacuum pump, a feed tank in a water batch, a condenser, an electronic balance connected to a personal computer, and a cooler. The feed water was heated by the water batch and the water vapor passed through the membrane and condensed in the condenser. The mass of water collected by the condenser was measured by the electronic balance. The degree of vacuum for the experiments was set to 80 mbar. Sodium chloride solution of 1,000 mg/L with the temperature of 70°C was used as the feed water. The operation conditions are summarized in Table 1.

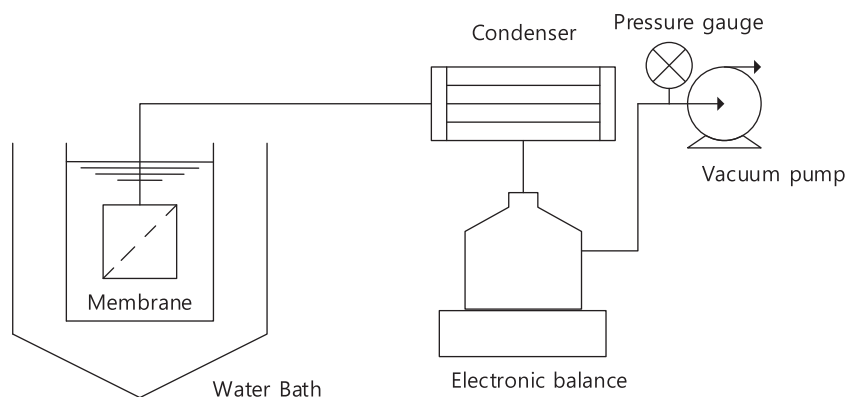


Fig. 1. Schematic diagram for MD experimental set-up.

Table 1
Operating conditions for MD

Operation parameter	Condition
Feed solution	3.5wt.% NaCl solution
Effective area	0.0125 m ²
Vacuum	0.8 bar
Feed temperature	70 °C

2.3. Method of wetting and dewetting

Prior to the dewetting experiments, MD membranes were intentionally wetted. Fig. 2 shows the schematics for wetting of MD membranes. First, the membrane was immersed in an ethanol solution for 5 min. Then, the surface of the membrane was washed using deionized water. After this step, the membrane was immersed into a vessel containing deionized water for 2 h to allow the replacement of ethanol in the pores with water.

The dewetting was carried out using high-temperature air flow. The experimental setup for dewetting is shown in Fig. 3. The high-temperature air flow was generated using a blower and a heater. A vacuum pump was used to help the air penetration into the pores. The temperature of the air was controlled by adjusting the power of the heater. The time for air flow was also adjusted.

2.4. LEP measurement

The LEP is a critical parameter for MD membranes because it represents the pressure over which liquid water can enter the membrane pores. Once the pores are filled with water, solutes may directly pass from the feed to the product stream, leading to their poor rejection. Accordingly, the operating pressure should not exceed the LEP of the MD membrane. Moreover, the LEP is an index for relative propensity of membrane wetting. If the LEP is high, the membrane is not easy to be wetted.

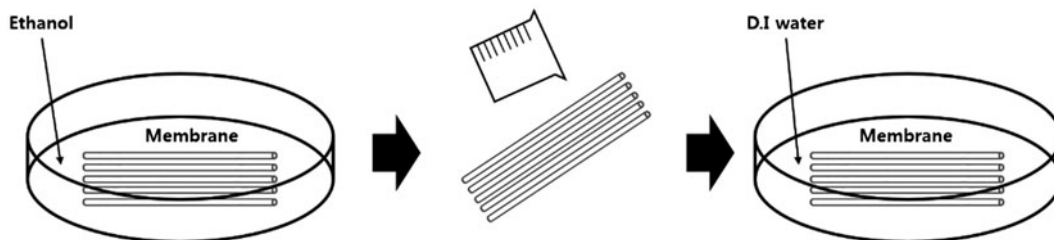


Fig. 2. A method for wetting of membrane.

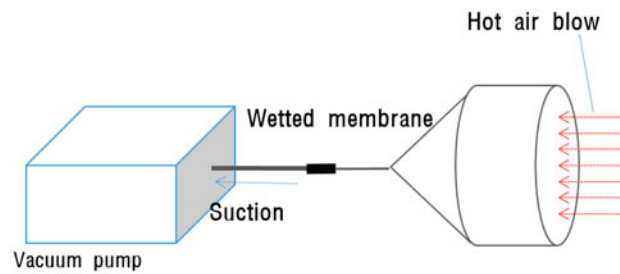


Fig. 3. Schematic diagram of dewetting device.

The relationship between the LEP and relevant system characteristics are described in the Laplace (Cantor) equation.

$$\text{LEP} = \frac{-2B\gamma \cos(\theta)}{r_{\max}} \quad (1)$$

where B is a geometric factor for which a value of 1 indicates circular pores, γ is the liquid surface tension, θ is the liquid–solid contact angle, and r_{\max} is the largest pore radius. However, it is difficult to accurately calculate the LEP using this equation.

In this study, the LEP of the membranes were directly measured using a device shown in Fig. 4. The system consists of a high-pressure nitrogen cylinder, a pressure regulator, a pressure vessel, a pressure gauge, and a membrane holder. The pressure applied to the membrane increases stepwise until the water penetrates the membrane. The measurements were triplicated to obtain reliable results.

2.5. Response surface methodology

RSM explores the relationships between several explanatory variables and one or more response variables [14]. The main idea of RSM is to use a sequence of designed experiments to obtain an optimal response. Experimental design and RSM were applied to optimize condition of dewetting. In this study, the

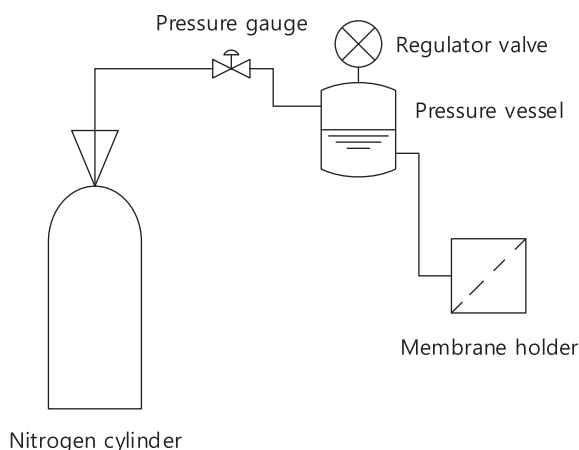


Fig. 4. Schematic diagram of LEP measurement device.

central composite design (CCD) was selected for the optimization of condition used for dewetting. This method is suitable for fitting a quadratic, surface and it helps to optimize the effective parameters with minimum number of experiments as well as to analyze the interaction between parameters. Each curve represents the evolution of dewetting by varying one variable in the extreme of the CCD model, with its pair variable equal to upper value (+1) and equal to low value (−1) [11]. The level of interaction of one variable on the other is represented between these two situations. A mathematical function is assumed for the response in terms of the significant independent variables. A quadratic model corresponding to the following second-order equation was built to describe the response:

$$Y = b_0 + \sum_i b_i X_i + \sum_i b_{ii} X_i^2 + \sum_{ij} b_{ij} X_i X_j \quad (2)$$

where Y is the response, b_0 is the constant coefficient, b_i is the linear coefficients, b_{ii} is the quadratic coefficients, b_{ij} is the interaction coefficients, and X_i and X_j are the coded values of the variables. In this work, a second-order polynomial equation was obtained using the uncoded independent variables as below:

$$Y = b_0 + b_1 X_1 + b_2 X_2 + b_{11} X_1^2 + b_{22} X_2^2 + b_{12} X_1 X_2 \quad (3)$$

The statistical significance of the models was justified through analysis of variance (ANOVA) for polynomial model with 95% confidence level, and the residual plots were used to examine the goodness of fit of the models. The quality of the fit polynomial model was also expressed by the coefficient of deter-

mination R^2 . Finally, optimum values of factors were obtained by determining a target in dedicated RSM program (response optimizer).

In this study, two factors including air temperature and air blowing time with five levels were employed for response surface modeling and optimization of dewetting condition.

3. Results and discussion

3.1. Application of RSM: the first set of experiments

To begin, the design of experiments were carried out using the CCD method. The experimental domains and the levels of the variables are given in Table 2. According to this, a total of 13 experiments were carried out to investigate the effect of dewetting conditions on dewetting efficiency. In each experiment, the LEP, water flux, and rejection were measured. The results are summarized in Table 3.

As the temperature changes from 40 to 80°C and the time changes from 5 to 25 min, the LEP varies between 2.37 and 2.72 bar. The flux and salt rejection range from 6.64 to 10.68 kg/m²-h and from 51.64 to 98.95%, respectively. These results suggest that the dewetting efficiency is sensitive to the temperature and time of the air flow. If the rejection is lower than 98%, the membrane is not fully dewetted. For instance, the dewetting at 40°C for 15 min (Run 9) showed the salt rejection of 51.64%, indicating that the dewetting of the membrane was not complete. On the other hand, the dewetting condition is not appropriate if the flux is lower than 10 kg/m²-h. For instance, the dewetting at 70°C for 20 min resulted in the water flux of 6.64 kg/m²-h, suggesting that the water permeability of the membrane was reduced after the dewetting.

3.2. Effect of dewetting condition: quantitative analysis

The experimental results in Table 3 were used to carry out quantitative analysis. A statistical analysis software (Minitab, USA) was used to derive regression

Table 2
Designed variables and their coded and actual values used for experimental design

Factor	Symbol	Actual value of coded levels				
		−1.414	−1	0	1	1.414
Temperature (°C)	X_1	40	50	60	70	80
Time (min)	X_2	5	10	15	20	25

Table 3
Design and result of experiments

Factor			Y_1	Y_2	Y_3
Run	Temperature (X_1)	Time (X_2)	LEP (bar)	Flux (kg/m ² h)	Salt rejection (%)
1	50	20	2.37	10.69	97.73
2	60	15	2.72	10.11	98.41
3	60	15	2.68	9.87	98.86
4	50	10	2.64	10.25	98.64
5	70	10	2.61	8.45	97.73
6	70	20	2.42	6.64	97.95
7	80	15	2.63	9.27	96.09
8	60	25	2.57	8.79	96.82
9	40	15	2.57	21	51.64
10	60	15	2.69	10.43	98
11	60	15	2.69	9.64	98.5
12	60	5	2.57	8.06	97.95
13	60	15	2.67	10.12	98.95

equations. For the LEP, the following equation was obtained:

$$Y_1 = -0.8 + 0.089X_1 + 0.96X_2 - 0.00057X_1^2 - 0.001X_2^2 - 0.0011X_1X_2 \quad (4)$$

where Y_1 is predicted response (LEP), X_1 is the temperature, and X_2 is the time. However, the R^2 value for RSM equation was only 58.4%, which suggests that the statistical importance of this equation is not high. This was attributed to the ranges of factors (temperature and time), which seem to be inappropriate.

Although the R^2 value is low, Eq. (2) is still useful to qualitatively understand the effect of dewetting conditions on the LEP value. Fig. 5 shows the effect of the temperature and time on the LEP after dewetting based on the previous analysis. The LEP increases with the increase of temperature and time. Above certain conditions, however, the LEP decreases even with the increase of temperature and time. This is attributed to the changes in membrane property under excessive application of air flow. The membrane may be deformed or damaged under those conditions. Accordingly, it appears that the dewetting conditions should be optimized to remove water from the

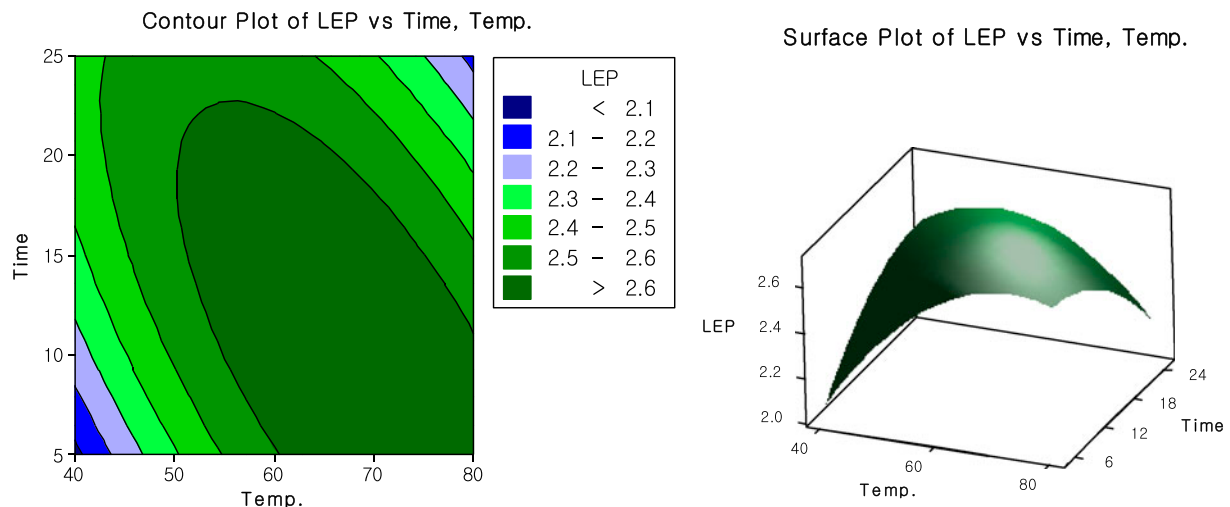


Fig. 5. Response surface plots of LEP (Temperature: between 40 and 80 °C; Time: between 5 and 20 min).

membrane pores and to prevent thermal damage by high-temperature air flow.

The results of the RSM analysis for water flux is shown in Fig. 6. The regression equation for water flux is given by

$$Y_2 = 54.8 - 1.56X_1 + 1.19X_2 + 0.012X_1^2 - 0.017X_2^2 + 0.011X_1X_2 \quad (5)$$

In this case, the R^2 value was 88.04%, which is significantly higher than that for the LEP. As shown in Fig. 6, the water flux is more sensitive to the temperature than the time. At low temperature, it is predicted that the

water flux is high, indicating that the dewetting is not sufficient and the water leakage occurs. At high temperature and long time for dewetting, the water flux is low due to the thermal deformation of membranes.

Fig. 7 shows the results of the RSM analysis for salt rejection. The regression equation for water flux is obtained by:

$$Y_3 = -158.2 + 7.93X_1 - 0.17X_2 - 0.06X_1^2 - 0.0075X_2^2 + 0.0057X_1X_2 \quad (6)$$

The R^2 value was 78.03%, which is not successful yet. Again, the salt rejection was highly dependent

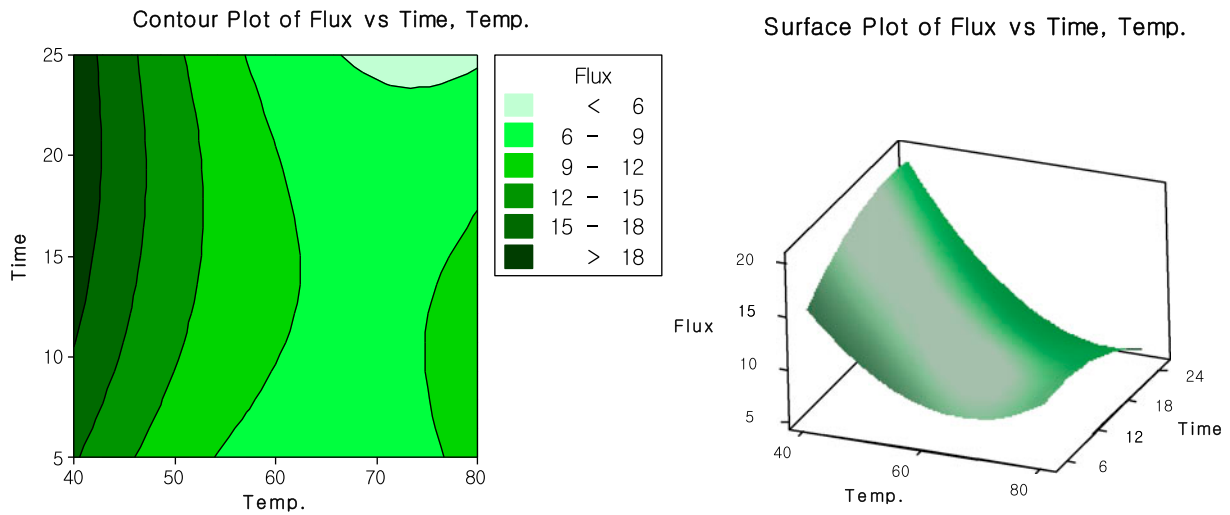


Fig. 6. Response surface plots of water flux (Temperature: between 40 and 80°C; Time: between 5 and 20 min).

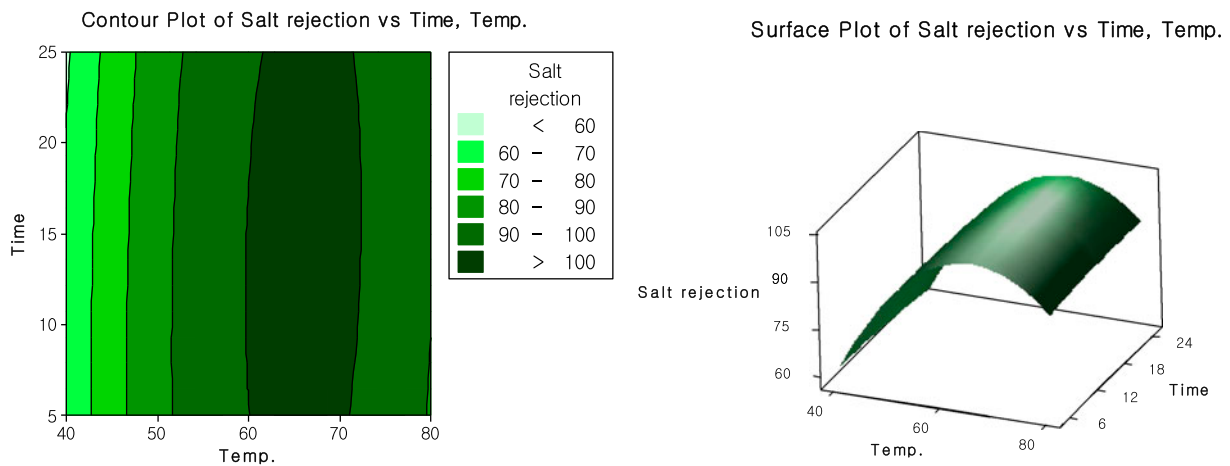


Fig. 7. Response surface plots of salt rejection (Temperature: between 40 and 80°C; Time: between 5 and 20 min).

on the temperature rather than the time. The maximum salt rejections were obtained where the temperature ranges between 60 and 70°C. The time for dewetting does not seem to be important in this case.

3.3. Analysis of membrane before and after dewetting

Based on the previous results, it seems that the deformation of membranes occurs at high-temperature conditions for dewetting. To confirm this, scanning electron microscopy was applied for the membranes before and after dewetting. The results are shown in Fig. 8. It is evident from the figures that the dewetting of membranes at 80°C resulted in the modification of membrane surface structure. Since the surface pores were reduced by the deformation, it is expected that the water flux decreases after dewetting at high temperature. Although it is not significant, the

dewetting at 60°C also altered the membrane surface. These results confirm the adverse effect of high-temperature air on the membrane surface structure.

3.4. Application of RSM: the second set of experiments

Although the previous RSM analysis was helpful for qualitative understanding of the effect of dewetting conditions on dewetting efficiency, it was limited due to low R^2 values. Accordingly, the experimental runs were redesigned to obtain quantitative correlations. Since the time was less important, the range was adjusted. The experimental domains and the levels of the variables are given in Table 4. The results for the design of experiments are also summarized in Table 5.

Based on the experimental design, the results were analyzed using the RSM, and an approximating function of the LEP was obtained by the following:

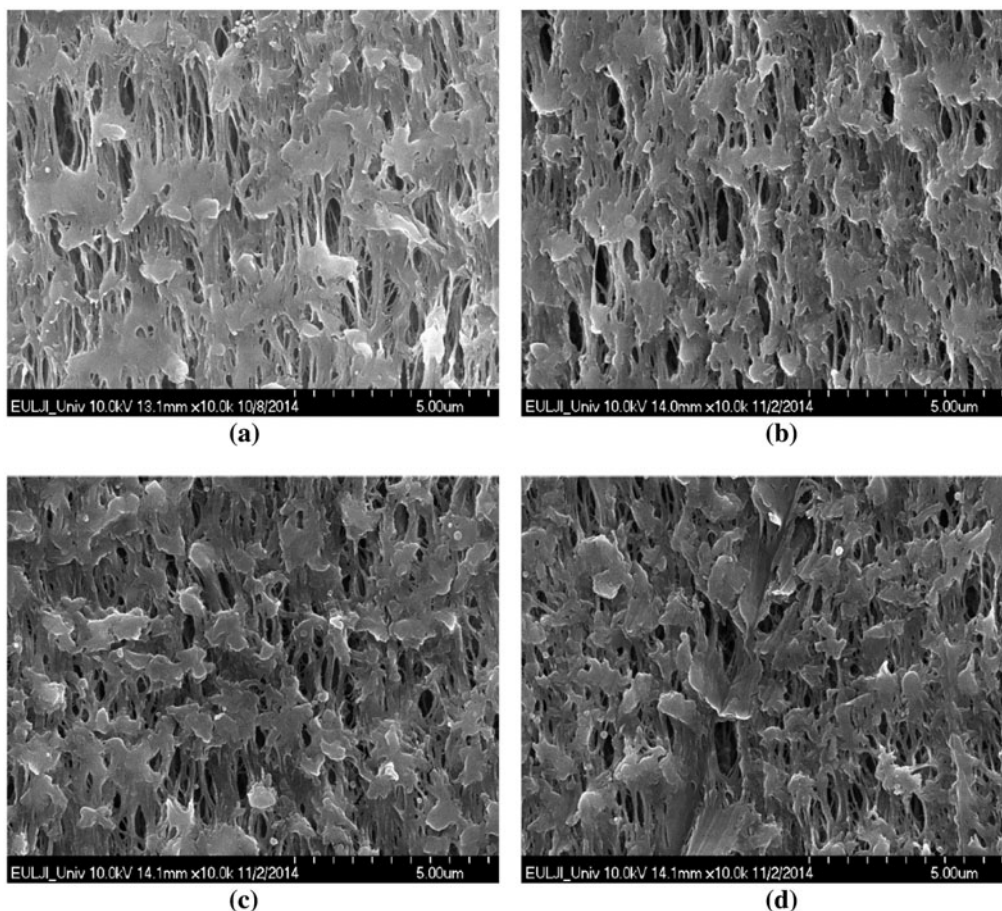


Fig. 8. SEM images for MD membranes (magnification: 10,000 times). (a) Original membrane, (b) membrane after dewetting at 40°C for 20 min, (c) membrane after dewetting at 60°C for 20 min, and (d) membrane after dewetting at 80°C for 20 min.

Table 4
Designed variables and their coded and actual values used for experimental design: second set

Factor	Symbol	Actual value of coded levels				
		-1.414	-1	0	1	1.414
Temperature (°C)	X ₁	40	50	60	70	80
Time (min)	X ₂	3	6	9	12	15

$$Y_1 = -13.83 + 0.218X_1 + 2.02X_2 - 0.0566X_2^2 - 0.0146X_1X_2 \quad (7)$$

In this case, the R² value was 94.43%, which is sufficiently high for quantitative analysis. A contour of constant LEP are shown as functions of the temperature and time in Fig. 9. As expected, the LEP initially increases and then decreases as the temperature and time increase. At low values for the temperature and time, the LEP was lower than 2.0 bar. At high values for the temperature and time, the LEP was also lower than the normal values. Based on this analysis, the optimum conditions occur between 60 and 70°C for temperature and between 8 and 12 min for time, respectively.

Table 5
Design and result of experiments

Run factors	Temperature (X ₁)	Time (X ₂)	Y ₁ LEP (bar)	Y ₂ Flux (kg/m ² -h)	Y ₃ Salt rejection (%)
1	60	15	2.71	10.45	97.73
2	60	9	2.71	10.11	98.18
3	70	12	2.64	8.1	97.36
4	60	9	2.71	10.72	97.95
5	40	9	1.98	170	20.41
6	60	9	2.68	11.1	98.09
7	50	6	2.12	80.6	34.91
8	80	9	2.69	9.42	96.45
9	60	9	2.7	10.45	98.55
10	70	6	2.68	9.12	97.14
11	60	3	2.33	47.4	50.91
12	50	12	2.68	10.45	96.09
13	60	9	2.69	9.89	98.64

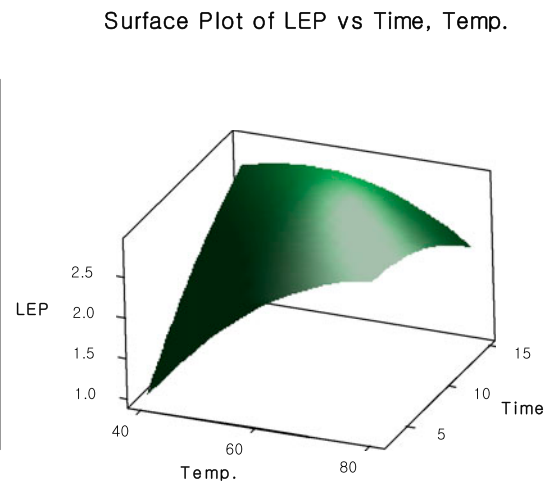
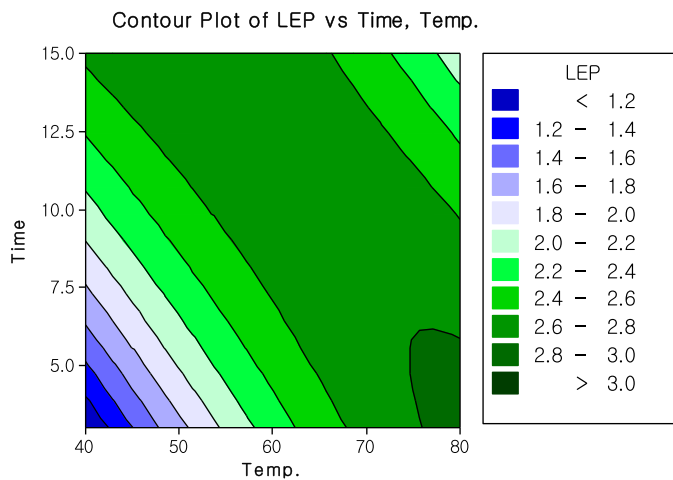


Fig. 9. Response surface plots of LEP (Temperature: 40–80°C; Time: 3–15 min).

The regression equations for water flux and salt rejection were also obtained from the RSM analysis:

$$Y_2 = 1301.94 - 32.1X_1 - 47.56X_2 + 0.2X_1^2 + 0.5X_2^2 + 0.57X_1X_2 \tag{8}$$

$$Y_3 = -736.1 + 18.34X_1 + 46.8X_2 - 0.1X_1^2 - 0.67X_2^2 - 0.5X_1X_2 \tag{9}$$

The R^2 values for water flux and salt rejection were 93.88 and 99.31%, respectively. The contours are shown in Figs. 10 and 11. Again, the optimum conditions were found 60°C for temperature 10 min for time in Fig. 12.

3.5. Verification of optimized conditions and predictive model

To confirm the adequacy of optimization, experiments were carried out under optimized conditions and the results were compared with the predicted values of model equation. The optimization reveals that LEP, water flux, and salt rejection were, 2.66 bar, 10.45 kg/m² h, and 98.56%, respectively. The results obtained from reproducibility experiments are within 99% of predicted values. This indicates the validity of the developed regression model of dewetting conditions.

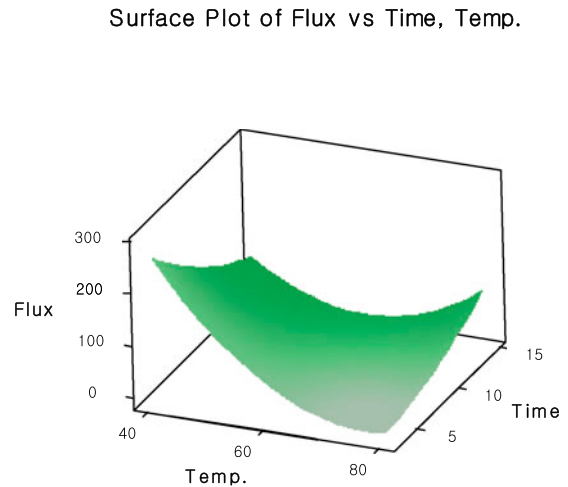
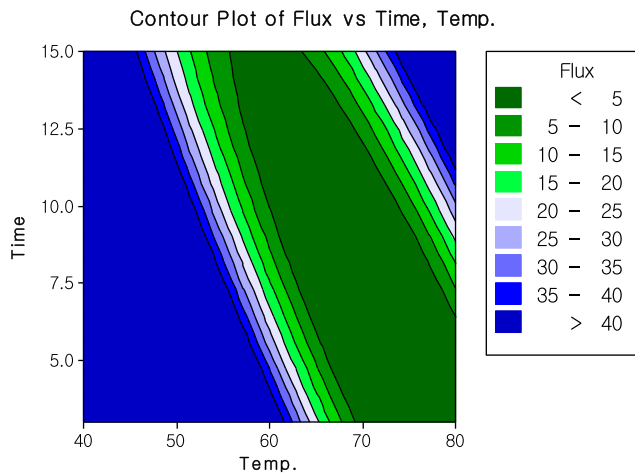


Fig. 10. Response surface plots of water flux (Temperature: 40–80°C; Time: 3–15 min).

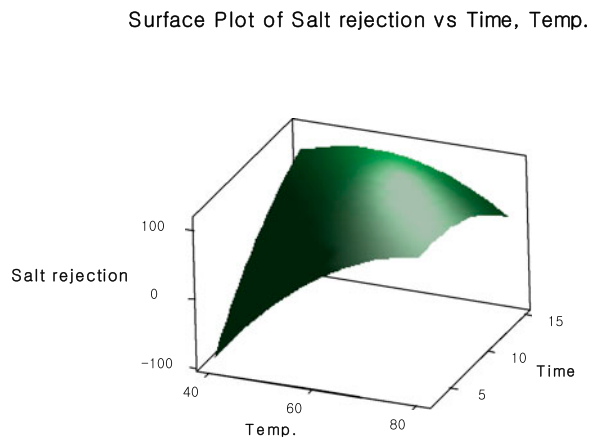
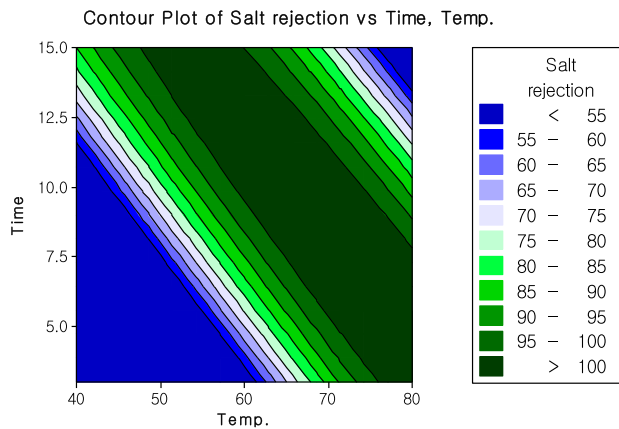


Fig. 11. Response surface plots of salt rejection (Temperature: 40–80°C; Time: 3–15 min).

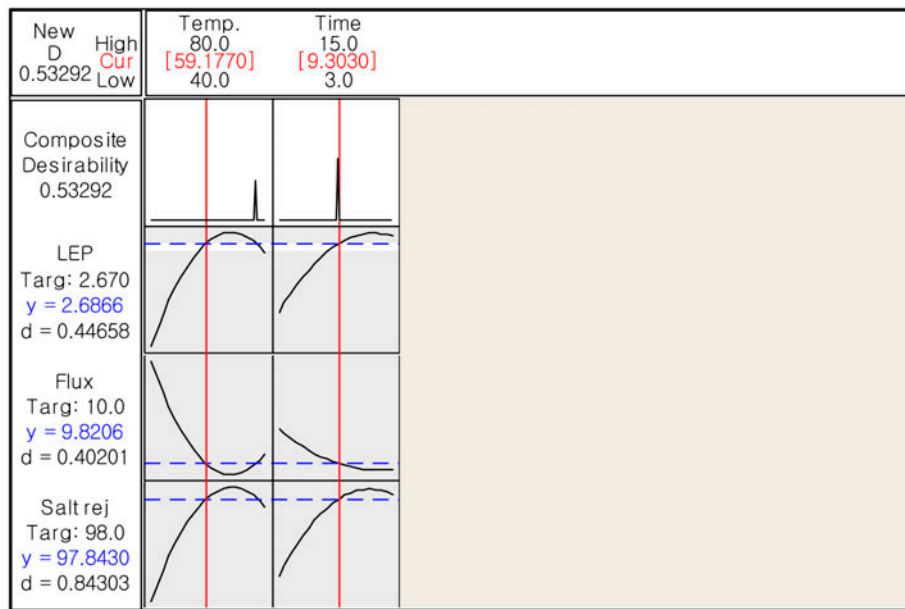


Fig. 12. Final optimization of dewetting conditions (Targeting of LEP: 2.67 bar; Flux: 10 kg/m²-h; Salt rejection: 98%).

4. Conclusions

In this study, a technique for dewetting of membranes using high-temperature air was applied to a laboratory-scale submerged VMD system. The following conclusions were withdrawn.

- (1) The high-temperature air was found to be effective to recover water flux and salt rejection for wetted membranes. The LEP measurement was useful to examine the dewetting efficiency even before the MD experiments.
- (2) The efficiency of dewetting by high-temperature air was sensitive to the operation parameters such as the temperature and time. Dewetting at low temperature and short time resulted in incomplete dewetting, leading to low salt rejection and low LEP. On the other hand, dewetting at too high temperature resulted in thermal deformation of membrane surface, leading to low flux and high LEP.
- (3) The deformation of membrane surface structure at high temperature (80°C) was confirmed by the SEM analysis.
- (4) The RSM was applied to explore the optimum conditions of temperature and time for the dewetting. The optimum temperature for dewetting is 60°C and the optimum time is 10 min.

Acknowledgments

This research was supported by a grant (code 131FIP-B065893-01) from Industrial Facilities & Infrastructure Research Program funded by Ministry of Land, Infrastructure and Transport of Korean government and also supported by Korea Ministry of Environment as Global Top Project (Project No. GT-14-B-01-003-0).

References

- [1] E. Drioli, A. Ali, F. Macedonio, Membrane distillation: Recent developments and perspectives, *Desalination* 356 (2014) 56–84.
- [2] E. Curcio, E. Drioli, Membrane distillation and related operations—A review, *Sep. Purif. Rev.* 34 (2005) 35–86.
- [3] A. Alkudhiri, N. Darwish, N. Hilal, Membrane distillation: A comprehensive review, *Desalination* 287 (2012) 2–18.
- [4] P. Wang, T.-S. Chung, Recent advances in membrane distillation processes: Membrane development, configuration design and application exploring, *J. Membr. Sci.* 474 (2015) 39–56.
- [5] A. Rom, W. Wukovits, F. Anton, Development of a vacuum membrane distillation unit operation: From experimental data to a simulation model, *CEPPI* 86 (2014) 90–95.
- [6] M. Ramezani-pour, M. Sivakumar, An analytical flux decline model for membrane distillation, *Desalination* 345 (2014) 1–12.
- [7] S. Chung, C.D. Seo, H. Lee, J.-H. Choi, J. Chung, Design strategy for networking membrane module

- and heat exchanger for direct contact membrane distillation process in seawater desalination, *Desalination* 349 (2014) 126–135.
- [8] L.D. Tijjng, Y.C. Woo, J.-S. Choi, S. Lee, S.-H. Kim, H.K. Shon, Fouling and its control in membrane distillation—A review, *J. Membr. Sci.* 475 (2015) 215–244.
- [9] S. Goh, J. Zhang, Y. Liu, A.G. Fane, Fouling and wetting in membrane distillation (MD) and MD-bioreactor (MDBR) for wastewater reclamation, *Desalination* 323 (2013) 39–47.
- [10] E. Guillen-Burrieza, R. Thomas, B. Mansoor, D. Johnson, N. Hilal, H. Arafat, Effect of dry-out on the fouling of PVDF and PTFE membranes under conditions simulating intermittent seawater membrane distillation (SWMD), *J. Membr. Sci.* 438 (2013) 126–139.
- [11] H.A.A. Rasha, B. Saffarin, Effect of temperature-dependent microstructure evolution on pore wetting in PTFE membranes under membrane distillation conditions, *J. Membr. Sci.* 429 (2013) 282–294.
- [12] L.F. Dumée, S. Gray, M. Duke, K. Sears, J. Schütz, N. Finn, The role of membrane surface energy on direct contact membrane distillation performance, *Desalination* 323 (2013) 22–30.
- [13] E. Guillen-Burrieza, A. Ruiz-Aguirre, G. Zaragoza, H.A. Arafat, Membrane fouling and cleaning in long term plant-scale membrane distillation operations, *J. Membr. Sci.* 468 (2014) 360–372.
- [14] A. Boubakri, A. Hafiane, S.A.T. Bouguecha, Application of response surface methodology for modeling and optimization of membrane distillation desalination process, *J. Ind. Eng. Chem.* 20 (2014) 3163–3169.